

Shipping and algae emissions have a major impact on ambient air mixing ratios of NMHCs and methanethiol on Utö island in the Baltic Sea

5 Heidi Hellén¹, Rostislav Kouznetsov¹, Kaisa Kraft², Jukka Seppälä², Mika Vestenius¹, Jukka-Pekka Jalkanen¹, Lauri Laakso^{1,3}, Hannele Hakola¹

¹Finnish Meteorological Institute, P.O. Box 503, FI-00101 Helsinki, Finland

²Finnish Environment Institute, Latokartanonkaari 11, FIN-00790 Helsinki, Finland

10 ³ Atmospheric Chemistry Research Group, Chemical Resource Beneficiation, North-West University, Potchefstroom 2520, South Africa

Correspondence to: Heidi Hellén (heidi.hellen@fmi.fi)

15 **Abstract.** Mixing ratios of highly volatile organic compounds were studied on Utö Island in the Baltic Sea. Measurements of non-methane hydrocarbons (NMHCs) and methanethiol ([unexpectedly found during the experiment](#)) were conducted using an in situ thermal desorption-gas chromatograph-flame ionization detector/mass spectrometer (TD-GC-FID/MS) from March 2018 until March 2019. The mean mixing ratios of NMHCs (alkanes, alkenes, alkynes, aromatic hydrocarbons) were at the typical levels for rural/remote sites in Europe and as expected the highest mixing ratios were measured in winter while in
20 summertime, the mixing ratios remained close to or below detection limits for most of the studied compounds. Sources of NMHCs during wintertime were studied using positive matrix factorization (PMF) together with wind direction analyses and source area estimates. Shipping was found to be a major local anthropogenic source of NMHCs with a 21% contribution. It contributed especially on ethene, propene and ethyne mixing ratios. Other identified sources were gasoline fuel (15%), traffic exhaust (14%), local solvents (6%), and long-range transported background (42%). Contrary to NMHCs, high mixing ratios
25 of methanethiol were detected in summertime (July mean 1000 pptv). The mixing ratios followed the variations of seawater temperatures and sea level height and were highest during the daytime. Biogenic phytoplankton or macroalgae emissions were expected to be the main source for methanethiol.

1 Introduction

30 Atmospheric NMHCs (non-methane hydrocarbons) are composed of light alkanes, alkenes, alkynes and aromatics with high vapor pressure. Together with compounds containing additional oxygen, nitrogen or other heteroatoms, they are also called volatile organic compounds (VOCs). NMHCs are emitted to the atmosphere due to fossil fuel or wood burning, solvent usage,

gas leakage etc. In the atmosphere NMHCs react with nitrogen oxides by means of hydroxyl radical reactions leading to the production of ozone. Ozone is a phytotoxic compound that is also harmful to health. Therefore, the EU has set limit values for ozone concentrations, and implements policies to reduce emissions of ozone precursors. During 1994-2020 the emissions of NMHC in the European Union decreased by ~58% (EMEP emission database, <https://www.ceip.at/webdab-emission-database>, last accessed 9.10.2023).

NMHCs were measured on Utö Island in the Baltic Sea in Finland during 1992-2007 by collecting air samples in stainless steel canisters twice a week for further analysis in the laboratory. The results of these measurements have been published in Laurila and Hakola (1996) and Hakola et al. (2006). These studies found a clear seasonal cycle of the NMHCs with the highest mixing ratios during winter. In this study, from March 2018 to March 2019, NMHCs were measured in the same location but at higher frequency, with a 2-hour time resolution and using in-situ gas chromatograph. With higher time resolution data, it is possible to study source the apportionment and source areas of measured NMHCs.

Positive matrix factorization (PMF) is commonly used for source studies of air pollutants (Sun et al. 2020). It has also been applied for NMHCs at different kinds of locations but only a few studies have used it on NMHCs at remote/rural sites (Leuchner et al. 2015, Lanz et al. 2009, Sauvage et al. 2009). Vestenius et al. (2021) applied PMF for more reactive biogenic VOCs in a boreal forest. At these kinds of environments photochemical aging must be considered when interpreting the results (Yuan et al. 2012). In this study, we use PMF combined with wind direction distributions and source area analyses to study sources of NMHCs in marine air on Utö Island in the Baltic Sea. In Northern Europe, the source areas of NMHCs have been studied earlier at a sub-Arctic site, i.e., Pallas, Finland (Hellén et al., 2015), where source area studies of NMHCs indicated that the EU was no longer a significant source area for NMHCs at that study site. The main source area was in Eastern Europe to the southeast of Pallas.

Together with other pollutants (e.g., particles, sulphur dioxide and nitrogen oxides) combustion in ship engines produces NMHCs and these emissions may have strong impacts on the air quality in coastal and marine areas (e.g., Viana et al. 2014, Tang et al. 2020). One aim of this study was to quantify the impact of shipping on mixing ratios of NMHCs in marine air in the Baltic Sea.

In the current publication we also study how frequently occurring phytoplankton blooms may affect the atmosphere. The Baltic Sea is a brackish, eutrophied, and non-tidal coastal sea with high concentrations of dissolved organic matter (DOM), where phytoplankton blooms occur frequently (Kahru and Elmgren, 2014). Kilgour et al., (2021) studied sulphur emissions during an induced phytoplankton bloom and they found that dimethylsulfide (DMS), methanethiol (CH_3SH), and benzothiazole ($\text{C}_6\text{H}_5\text{N}_2\text{S}$) account for on average over 90% of total gas-phase sulphur emissions. While there are lots of studies on the mixing ratios of DMS, less is known about the other sulphuric compounds in marine air. Lawson et al. (2020) measured methanethiol and DMS in the air over remote parts of the southwest Pacific Ocean and Novanak et al. (2022) their fluxes and mixing ratios in marine air on the coast of California, US (Novanak et al. 2022). Sulphur compounds are oxidized in the air forming sulphur dioxide (SO_2). In the air, SO_2 is further oxidized producing sulphuric acid, which participates in new particle and cloud formation in the air. Atmospheric NMHCs (non-methane hydrocarbons) are composed of light alkanes, alkenes, alkynes and

aromatics with high vapor pressure. Together with compounds containing additional oxygen, sulphur or other heteroatoms, they are also called volatile organic compounds (VOCs). NMHCs are emitted to the atmosphere due to fossil fuel or wood burning, solvent usage, gas leakage etc. (e.g. Ge et al. 2024). Some VOCs (e.g. isoprene and monoterpenes) are mainly emitted from biogenic sources (Guenther et al. 2012). In the atmosphere NMHCs react with nitrogen oxides by means of hydroxyl (OH) radical reactions leading to the production of ozone. Ozone is a phytotoxic compound that is also harmful to health. Therefore, the EU has set limit values for ozone concentrations, and implements policies to reduce emissions of ozone precursors. During 1994-2020 the emissions of NMHC in the European Union decreased by ~58% (EMEP 2023).

While NMHC mixing ratios have been monitored already for decades at several locations in Europe and their emissions are reported to the data bases (e.g. EMEP 2023, Ge et al. 2024), less is known on the marine areas and impacts of shipping on NMHCs mixing ratios. Together with other pollutants (e.g., particles, sulphur dioxide and nitrogen oxides) combustion in ship engines produces NMHCs and these emissions may have strong impacts on the air quality in coastal and marine areas (e.g., Viana et al. 2014, Tang et al. 2020).

In Northern Europe, the source areas of NMHCs have been studied earlier at a sub-Arctic site of Pallas, Finland (Hellén et al., 2015), where source area studies of NMHCs indicated that the EU was no longer a significant source area for NMHCs at that study site. The main source area was in Eastern Europe to the southeast of Pallas. However, source apportionment was not studied. Positive matrix factorization (PMF) is commonly used method for source apportionment studies of air pollutants (Sun et al. 2020). It has also been applied for NMHCs at different kinds of locations but only a few studies have used it on NMHCs at remote/rural sites (Leuchner et al. 2015, Lanz et al. 2009, Sauvage et al. 2009). Vestenius et al. (2021) applied PMF for more reactive biogenic VOCs in a boreal forest. At these kinds of environments photochemical aging must be considered when interpreting the results (Yuan et al. 2012).

Missing OH reactivity (up to 3.5 s^{-1}) found in oceanic regions worldwide clearly indicates that there is also a significant amount of additional currently unidentified reactive compounds emitted at marine areas (Thames et al. 2020). Fluctuations in missing reactivity correlate with dimethylsulfide (DMS) and sea surface temperature. DMS is known to be emitted by marine biota, but less is known on other sulfuric compounds (Yu and Li 2021). In the atmosphere organic sulphur compounds undergo oxidation to form sulphur dioxide (SO_2), which is further oxidized to produce sulfuric acid and sulphate aerosols. These aerosols influence cloud radiative properties, impacting climate (Hopkins et al. 2023). At coastal areas, sulphur compounds may also impact air quality. Better knowledge on the marine sulfuric emissions is essential also for evaluating the consequences of reduced SO_2 emissions from shipping. While lower emissions are anticipated to enhance air quality, there is a possibility of adverse effects on climate (Sofiev et al. 2018).

One of the potential candidates to explain this discrepancy is methanethiol. Due to its high reactivity with OH radicals, it is a promising candidate for the missing reactivity found in marine areas. Methanethiol is known to be emitted from phytoplankton, but the factors that control its production and emission rates are not well understood (Kilgour et al. 2022, Novak et al. 2022). It is formed in the seawater from the same precursor metabolite, dimethyl sulfoniopropionate (DMSP) as DMS (Kiene and Linn, 2000). In addition to phytoplankton, cyanobacteria is also noted as a source of methanethiol (Watson and Jüttner 2016).

Formatted: Not Highlight

In the atmosphere, methanethiol oxidizes with hydroxyl (OH) radicals seven times faster than DMS (Kilgour *et al.* 2022) and OH oxidation of methanethiol produces SO₂ with almost unity yield (Novak *et al.* 2022). There is very little information on atmospheric mixing ratios of methanethiol. Lawson *et al.* (2020) and Novak *et al.* (2022) measured mean mixing ratios of ~20 pptv in the SW Pacific Ocean and at the Scripps Institution of Oceanography in La Jolla, CA, USA, respectively. Due to high reactivity of the methanethiol, its mixing ratios are expected to remain low, even with relatively high emissions and therefore VOC monitoring networks with marine stations (e.g. Global Atmospheric Watch programme and ACTRIS) may have overlooked it. Even with mean mixing ratio of ~20 pptv, Novak *et al.* (2022) estimated that methanethiol could be a source of up to 30% of the SO₂ formed in the marine boundary layer in coastal California.

The aim of this study was to characterize the most volatile organic compounds in more detail in marine air in the Baltic Sea. Since terrestrial anthropogenic sources of NMHCs are relatively well-known, we focused on quantifying the impact of shipping on their mixing ratios. NMHCs containing 2 to 9 carbon atoms were measured at the same location on Utö Island in the Baltic Sea as in our previous studies (Laurila and Hakola 1996 and Hakola *et al.* 2006). In these earlier studies, air samples were systematically collected twice a week using stainless steel canisters, followed by detailed laboratory analysis. Now with in-situ measurements and higher (2-hour) time resolution, it was possible to study source apportionment and source areas of measured NMHCs in more detail and to use PMF combined with wind direction distributions and source area analyses. Given the high reactivity observed in marine areas, which cannot be attributed to currently known anthropogenic or biogenic compounds (Thames *et al.*, 2020), our objective was also to explore and identify novel compounds. During the measurements we detected an additional peak, which was identified as methanethiol. Results on methanethiol mixing ratios and its possible sources are presented to show the need for more studies on this compound.

2 Experimental setups

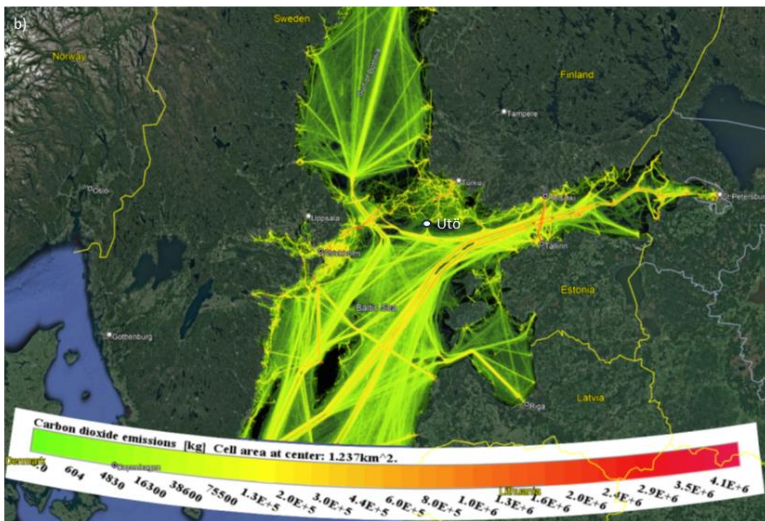
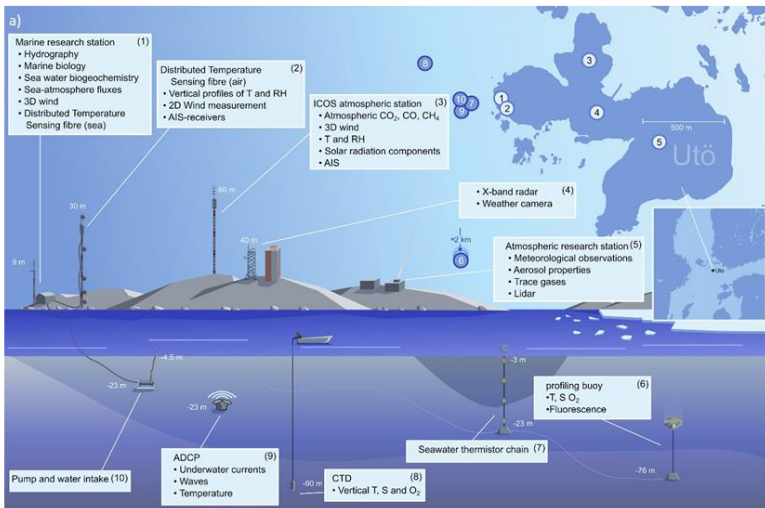
2.1 Measurement site

The Utö Atmospheric and Marine Research Station of the Finnish Meteorological Institute (59° 46'50N, 21° 22'23E) is located at the outermost edge of the Archipelago Sea, facing the Baltic Sea proper. The station provides an excellent possibility to observe marine biogenic emissions with minimal interference from terrestrial sources. The station produces real-time, high-frequency measurements of the physical, chemical and biological features of the water column and atmospheric concentrations of trace gases and aerosols (Fig. 1a; Laakso-Laakso *et al.*, 2018; Kraft *et al.*, 2021; Honkanen *et al.*, 2018, 2021, 2023; Rautiainen *et al.*, 2023).

Formatted: Default Paragraph Font

135

140



145 **Figure 1: a) Description of the Utö marine research station and b) predicted CO₂ emissions from ships sailing the Baltic Sea during 2022 (map © 2023 Google - Image Landsat / Copernicus). The main shipping routes are coloured according to emissions in relative mass units per unit area.**

2.2 Measurements of NMHCs and methanethiol

150 The samples were collected from a 9 m long mast (inlet 12 m above sea level, Fig. 1, Marine research station 1) with flow rate of ~2.2 L min⁻¹. The mast is located approximately 5 meters from the sea on the western edge of Utö island. A subsample was collected to a gas-chromatograph through a heated line. An in-situ thermal desorption unit (Unity 2 + Air Server 2, Markes International Ltd.) connected to a gas chromatograph (Agilent 7890) with a mass spectrometer (Agilent 5975C) and a flame ionization detector (TD-GC-MS/FID) was used. Two columns (HP-1, 50 m*0.22 mm*1 µm and Al/Na₂SO₄ PLOT, 50 m*0.32
155 mm) were connected using an Agilent Deans switch. Samples were taken every other hour from a 35 m long fluorinated ethylene propylene (FEP) inlet (1/8 inch I.D.) located on the 9 m long mast. An extra flow of 2.2 L min⁻¹ was used to avoid losses of the compounds on the walls of the inlet tube. Samples were collected directly from this ambient air flow through a Nafion drier into the cold trap (U-T17O3P-2S, Markes International Ltd.) of the thermal desorption unit. The sampling time was 30 min and the sampling flow through the cold trap 20 ml min⁻¹. All the lines and valves in the thermal desorption unit
160 were kept at 200°C. During sampling, the cold trap was kept at -30°C. For desorption, the cold trap was heated to 300°C for 3 minutes and flushed with a helium flow of 10 ml min⁻¹. Every 50th sample was a calibration sample. The calibration gas (National Physical Laboratory, 30 VOC mix) contained C₂-C₈ alkanes, C₂-C₅ alkenes, C₆-C₉ aromatic hydrocarbons, ethyne and isoprene at a ~4 ppb level. [Compounds detected and quantified were ethane, ethene, ethyne, propane, propene, n-butane, i-butane, n-pentane, i-pentane, 2-methylpentane, benzene, toluene, ethylbenzene, o-xylene, p/m-xylene and methanethiol.](#)
165 [Mixing ratios of the other NMHCs in the calibration gas remained below detection limits.](#)

In spring and ~~summer~~summer, we detected an unknown compound on the flame-ionization detector. It was later identified as methanethiol. Methanethiol was not included in the used standard mixture, but it was later identified based on an authentic standard (Linde gas/BOC, 5 component mix at a 10 ppm level) and it was also detected from cyanobacteria culture samples grown in the laboratory. It was calibrated as close eluting pentane and corrected based on carbon number.

2.3 Positive matrix factorization (PMF) modelling

The Utö winter NMHC dataset was analysed using EPA PMF version 5.0. PMF (Positive matrix factorization) which is a receptor modelling tool that is widely used in source apportionment of air pollution (Hopke, 2016; Hopke et al., 2020). PMF
175 decomposes the measured time series data matrix into two matrices, i.e., factor contributions and factor profiles and then uses a chemical mass balance equation to find a number of user specified factors (potential sources) that affect the measured species' concentration at the receptor. The results are constrained to be non-negativity for the factor profiles and non-significant

negativity for the factor contributions. VOC concentrations and especially biogenic VOC emission profiles may change quite rapidly in the atmosphere on the way from emissions to the receptor site due to the high reactivity of VOCs. Prior works on source apportionment of biogenic VOCs have shown that PMF is a valuable tool also for this kind of data (e.g., Vestenius et al., 2021). Even though studied anthropogenic NMHCs have longer atmospheric lifetimes than those of biogenic VOCs, their ratios may still vary during the transport, and this has to be taken into account while interpreting the results.

All compounds quantified, except p/m-xylene and methanethiol, were used for the PMF analyses. Methanethiol remained below detection limit during the winter months and p/m-xylene comprised < 2% of the total detected VOC mixing ratio.

Uncertainty calculations for the PMF model were made according to Polissar et al. (1998). The expanded measurement uncertainty (U) was estimated from partial uncertainties of analytical precision, standard preparation, and sampling flow. As PMF does not tolerate missing values in the data matrix, missing values (e.g., missing species in the sample) were replaced by species median with their uncertainties multiplied by ten, so that this “synthetic” data would not have effect on the model resolution. Values below detection limit (<LOD) were replaced by 0.5*LOD and their respective uncertainties were set to 5/6*LOD. Species were categorized as “strong”, “weak” or “bad” using their sample to noise ratios. S/N species with ratios over 2 were generally categorized as “Strong”, and species with S/N values between 0.2 and 2 were generally categorized as “weak.” Species with S/N values less than 0.2 were categorized as “bad” and were removed from the model. Weak categorization increases the species’ uncertainty by the factor of three. However, only three of the 14 modelled species; ethane, ethyl benzene and toluene were categorized as “Strong”, the other 11 species were categorized as “weak” due to their low S/N ratio. Uncertainty analyses of the model results were made using bootstrapping. The factor contributions (time series) were combined with local wind data using the OpenAir software package in R (Carslaw, 2018). A conditional bivariate probability function (CBPF) was used to estimate the conditional probabilities of source directions and distance from the receptor using local wind measurements. CBPF takes wind speed into account as a third variable in addition to concentration and wind direction and gives a probability of direction and likely distance of high factor contributions (potential source). In CBPF, the 75th percentile was used as threshold value so that the analysis gives a probability of direction and likely distance of highest factor contributions.

2.4 Source area estimates

Adjoint atmospheric dispersion simulations were used to identify the source areas for the samples collected during the measurements. The method is quite similar to the one used by Meinander et al. (2013), Hellén et.al. (2015) and Meinander et al. (2020), but for the sake of completeness, we briefly describe it below.

The simulations were performed with SILAM v5_8 (System for Integrated modeLing of Atmospheric coMposition <http://silam.fmi.fi>, accessed on 21.8.2023). This system incorporates a Eulerian non-diffusive transport scheme (Sofiev et.al., 2015). The model has been extensively validated for a variety of atmospheric dispersion and source inversion problems on a regional and global scale (Petersen et. al., 2019; Kouznetsov et.al. 2020)

The model was driven with the meteorological fields from ERA-5 (Hersbach et. al. 2020) at the resolution of 0.25x0.25 degrees. Adjoint simulations were made on a 0.5°x0.5° resolution grid, 8 vertical layers with varying thicknesses, spanning from 30 m at the surface to 2000 m at altitudes up to 6 km. For each of the about 900 samples collected, the model was integrated for six days backwards in time on a domain covering northern Europe. The resulting fields of sensitivity distribution (also known as footprints or retroplumes) were aggregated in time and stored for further analysis.

Each measured sample combines contributions from spatially and temporally distributed sources. Adjoint simulations allow for reconstructing a 4D sensitivity pattern of each sample to the location of a source in space and time. Combining the sensitivities with the sampled values one can infer the likely source areas for a specific variable. Since the individual observed compounds are highly correlated in the samples in this study, we used the concentrations of the PMF factors, rather than concentrations of individual compounds. For each of the factors, the retroplumes were aggregated for below the 20th percentile and above the 80th percentile to get a typical “clean”-sample source area and “polluted”-sample source areas. The aggregated retroplumes show the relative sensitivity of the corresponding samples to various locations of the emission source. The areas that are high for polluted samples, but low for clean ones are likely the origin of the specific factor.

2.5 Complementary data

Total phytoplankton biomass was obtained using imaging flow cytometry. An Imaging FlowCytobot (IFCB, McLane Research Laboratories, Inc., United States) was connected to the Utö station’s flow through system, taking a 5-mL sample approximately every 20 minutes. A chlorophyll *a* trigger was used to target the phytoplankton community (detailed explanation of the sampling system in Kraft et al. 2021). The data was classified using a Convolutional Neural Network classifier and image specific biovolumes were computed (Moberg and Sosik 2012, Kraft et al. 2022). The total phytoplankton biomass was calculated by summing up the total biovolumes of all classes, including also unclassified images, and converting the total biovolume ($\mu\text{m}^3 \text{mL}^{-1}$) to total biomass ($\mu\text{g L}^{-1}$) by assuming a plasma density of 1 g cm⁻³ (CEN, 2015).

The used meteorological data and ozone (O₃), sulphur dioxide (SO₂), particulate matter <2.5 μm (PM_{2.5}) and nitrogen dioxide (NO₂) concentration data is available at the Finnish Meteorological Institute open access data portal (<https://en.ilmatieteenlaitos.fi/download-observations>, last accessed 21.6.2023). The data were collected at a close by atmospheric research station on Utö island (Fig. 1a). Temperature and wind speed and direction were measured by the Automatic Weather Station. The concentration of NO₂ was measured by Thermo Electron 42i-TL analyzer, O₃ by an ambient air O₃ monitor (TEI 49i), SO₂ by Thermo Electron 43i TLE analyzer and PM_{2.5} by Thermo 5030 SHARP analyzer all produced by Thermo Fischer Scientific, Waltham, US.

Sea surface temperature was measured at a wave buoy 60 km to the South-West of Utö with a Datawell DWR4 Waverider buoy. Sea level height at Utö was interpolated from tide gauge observations at Föglö (62 km from Utö) and Hanko (90 km from Utö). The values are given relative to the theoretical mean sea level.

Formatted: Subscript

Formatted: Subscript

Formatted: Subscript

Formatted: Subscript

245 Carbon dioxide (CO₂) emissions originating from ship traffic over the Baltic Sea were used for presenting main shipping routes (Fig 1b). The emissions were modelled using the Ship Traffic Emission Assessment Model (STEAM), which uses Automatic Identification System data to describe ship traffic activity. The method is presented elsewhere (Jalkanen, 2009; Jalkanen et al., 2012; Johansson et al., 2017).

Formatted: Finnish

Field Code Changed

Formatted: Finnish

250 3 Results and discussion

3.1. ~~Seasonal variations~~Mixing ratios of NMHCs

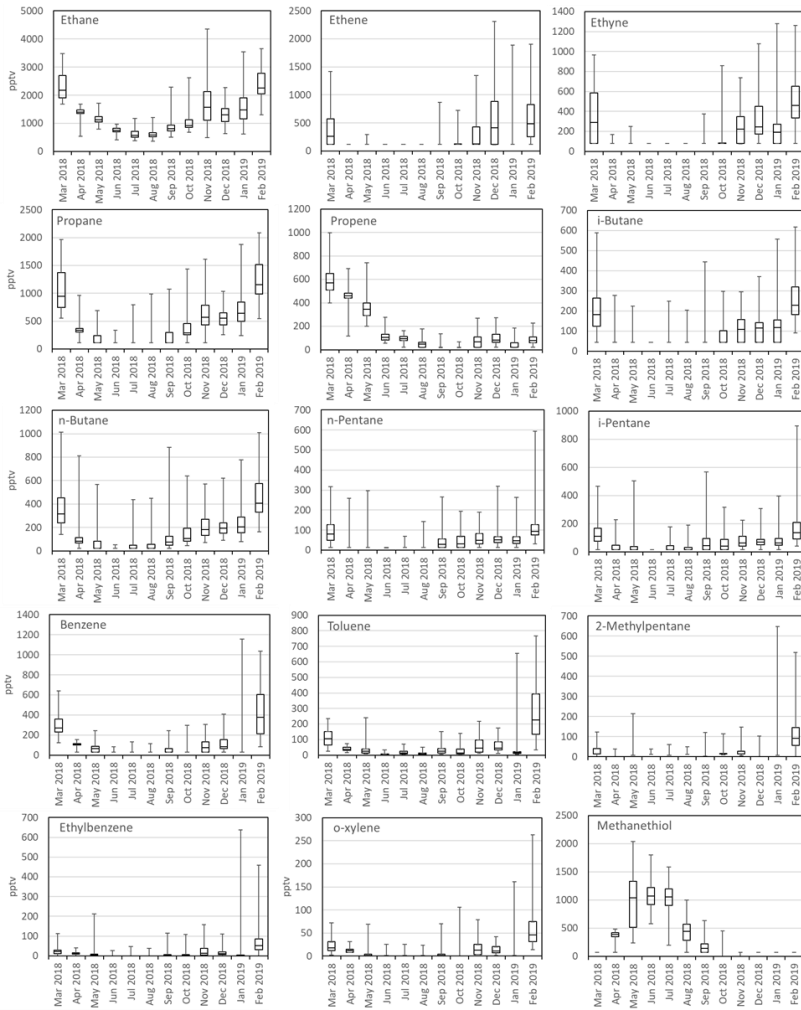
255 ~~The mean mixing ratios were at typical levels for rural/remote sites in Europe (Solberg et al. 2020). Ethane and propane were clearly the most abundant NMHCs detected, contributing mean percentages of 43% and 15%, respectively, to the total NMHC mixing ratio. The mean contribution of aromatic hydrocarbons (benzene, toluene, ethylbenzene, xylenes) was only 8%.~~

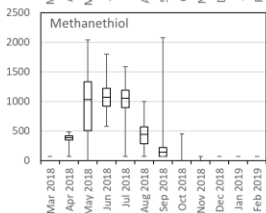
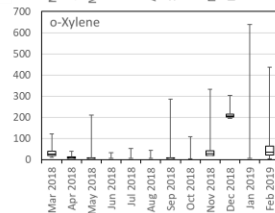
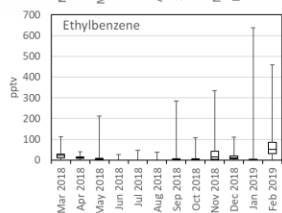
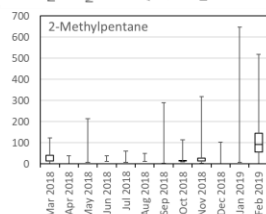
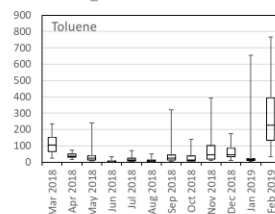
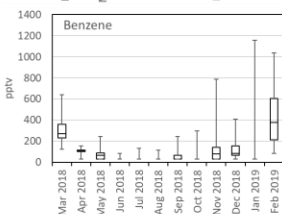
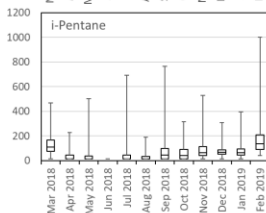
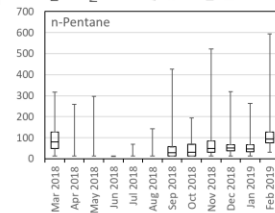
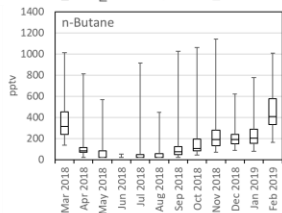
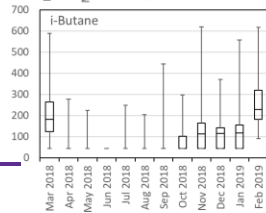
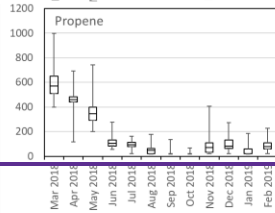
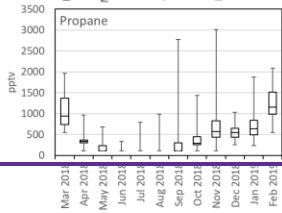
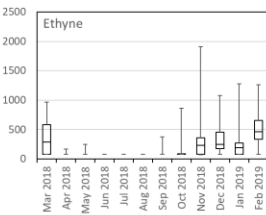
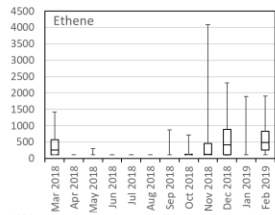
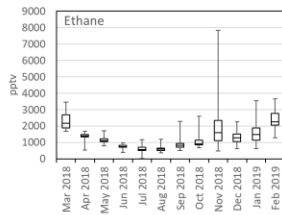
The seasonal variations of NMHCs followed a well-known cycle with maximum mixing ratios during the dark wintertime and minimum mixing ratios during summer, when mixing ratios of many compounds were below detection limits due to effective sink reactions with OH radicals (Fig. 2). Generally, the more reactive the compounds are, the larger the amplitude between summer and winter mixing ratios is. ~~The mean mixing ratios were at typical levels for rural/remote sites in Europe (Solberg et al. 2020).~~

260 ~~NMHCs has been measured on Utö Island in the Baltic Sea in Finland during 1992-2007 by collecting air samples in stainless steel canisters twice a week for further analysis in the laboratory (Laurila and Hakola 1996, Hakola et al. 2006). These studies found also a clear seasonal cycle of the NMHCs with the highest mixing ratios during winter. The seasonal cycle of methanethiol is contrary to the other VOCs as expected, since it is of biogenic origin and not emitted in wintertime.~~

Formatted: Font: Not Bold

Formatted: Font: Bold





270 **Figure 2: Monthly mean box and whisker plots of measured mixing ratios (pptv). The boxes represent second and third quartiles and the vertical lines in the boxes median values. The whiskers show the highest and the lowest measurements. Number of data points for each compound was 2175-2188. Values <LOD were marked as 0.5*LOD.**

3.2 Source apportionment of NMHCs

275 In PMF modelling, different combinations of 4 to 7 source factor solutions were tested. The most reasonable and interpretable results were obtained by a 5-factor solution, which was chosen for further investigation. Also, bootstrapping showed acceptable results to all factors for this solution, with no swaps for factors 1 to 4 and 95% mapping for F5, which is well within the acceptable range (80%). One of the factors represents regional background air and the other four factors were interpreted as ship, local solvent, gasoline, and traffic exhaust emissions as represented in Table 1 and described below. For PMF analysis, we could only use winter data since the mixing ratios of many of the compounds were very low or below detection limits during other times. The profiles of factors are not expected to directly represent the profiles of real emissions, since most of 280 these emissions are transported to the site over long distances, and during transportation NMHCs are oxidized with different rates, which means that the ratios of the compounds may change. This has been considered when interpreting the results. Ethane has a relatively high contribution to all factors (Fig. 3a). Ethane is the longest living NMHC [in the atmosphere](#) and has the highest mixing ratios. Background factor F3 is a major contribution factor for ethane (Fig. 3b). Due to the high mixing ratios of ethane compared to other compounds (Fig. 2), small changes in ethane mixing ratios (even within uncertainties) may 285 result in high contributions to the other factors. This has also been considered when interpreting the results.

Table 1: Identification of the PMF factors and the mean contribution to the NMHC mixing ratios measured at the site.

Factor	Name	Driver	Contribution
F1	Gasoline fuel	Butane, pentanes	15%
F2	Traffic exhaust	Aromatic hydrocarbons	14%
F3	Background	Ethane, propane, stable contribution	42%
F4	Ship emissions	Ethene, propene, ethyne	21%
F5	Local solvent	Ethylbenzene, o-xylene	6%

3.2.1 Identification of the PMF factors

290 Factor 1 (F1) was identified as gasoline fuel emissions. The factor had high contribution to butanes and pentanes (Fig. 3). These compounds are known to make a major contribution on the NMHC emissions of gasoline fuel and especially evaporated

295 gasoline (Hellén et al. 2006). Wind direction distribution indicated that the main source for this factor was further away to the east of the measuring site (Fig. 4). This direction includes the main harbours in the Gulf of Finland and the city of Saint Petersburg. This is supported by the sensitivity maps (Fig. 5). The maps corresponding to the clean samples for F1 (gasoline) have clear gaps over Russia and the southern shore of the Gulf of Finland, which correspond to high values in the polluted maps (Fig. 5ab). These areas likely contribute to high concentrations of this factor.

300 Factor 2 (F2) was a traffic exhaust emission factor. It was characterized by the strong contribution of aromatic hydrocarbons (Fig. 3), which are known to be major compounds in traffic exhaust emissions (e.g., Hellén et al. 2006, Wang et al. 2020, Wu et al. 2020a). This factor made a high contribution especially in the beginning of February during high wind speeds (Fig. 6). Wind direction distribution indicated that the main source was to the east of Utö in the direction of Saint Petersburg (Fig. 4). Sensitivity maps of F2 showed very similar source areas as for F1 (gasoline) with contribution from Russia and the southern

305 shore of the Gulf of Finland, except that it also contains a substantial contribution from the Baltic states (Fig. 5). Factor 3 (F3) was identified as long-range transported background air with a high contribution of the longest living NMHCs, ethane and propane (Fig. 3). The contribution of the factor over time was relatively stable compared to other factors (Fig. 6) and the highest contribution of the measured NMHCs, 42%, came within this factor. Wind direction distribution was more scattered as expected for the regional background (Fig. 4), but the main source area was to the west and north-west from the site. The close by shipping routes going to the Gulf of Bothnia and between cities of Turku (Finland) and Stockholm (Sweden)

310 are in that direction and ships running on those routes use liquified natural gas (LNG), which is known to have ethane and propane emissions (Anderson et al. 2015) and could be influencing this factor as well. Also, sensitivity maps indicated that F3 got most of its contribution from Finland and Sweden, and much less contribution from the Baltic states and Russia (Fig. 5). Factor 4 (F4) was identified as a shipping emission factor. It was characterized by the high contribution of ethene, propene and ethyne, which are major NMHCs in ship emissions (Bourtsoukidis et al., 2019; Wu et al., 2020b). The variation of the factor contribution followed the variation of NO₂ and PM_{2.5} (Fig. 6). Based on the wind direction distribution the main source area coincided with the main ship route going to the Finnish and Russian harbours in the Gulf of Finland (Fig. 1b). Sensitivity maps of air masses (Fig. 5) also indicated a main contribution from southern and south-eastern sectors with quite uniform directional spawn. This ship emission factor made a 21% contribution to the total measured NMHCs.

315 Factor 5 was interpreted as a local solvent factor. It was a significant source only of ethylbenzene and o-xylene (Fig. 3b). These compounds are well-known solvents, e.g., in paints and coatings (e.g., Castano et al. 2019, Song and Chun 2021). However, F5 contribution to the total measured NMHCs was low, only 6%. The wind direction probabilities indicated the local origin of the source; to the direction of the village and harbour of Utö island during low wind (Fig. 4). In November when the wind direction changes to the North contribution of this local factor decreases. (fig 6). Based on the sensitivity maps (Fig.

320 5) F5 had a similar pattern as F4 with a much narrower high-contribution sector in south-eastern direction from the measurement site.

Formatted: Not Highlight

The findings of the sensitivity maps were consistent with the wind analysis, being more specific for distant sources (F1-F3), for which the large-scale trajectories are important, and much less specific for local sources whose contribution is primarily controlled by local winds.

330

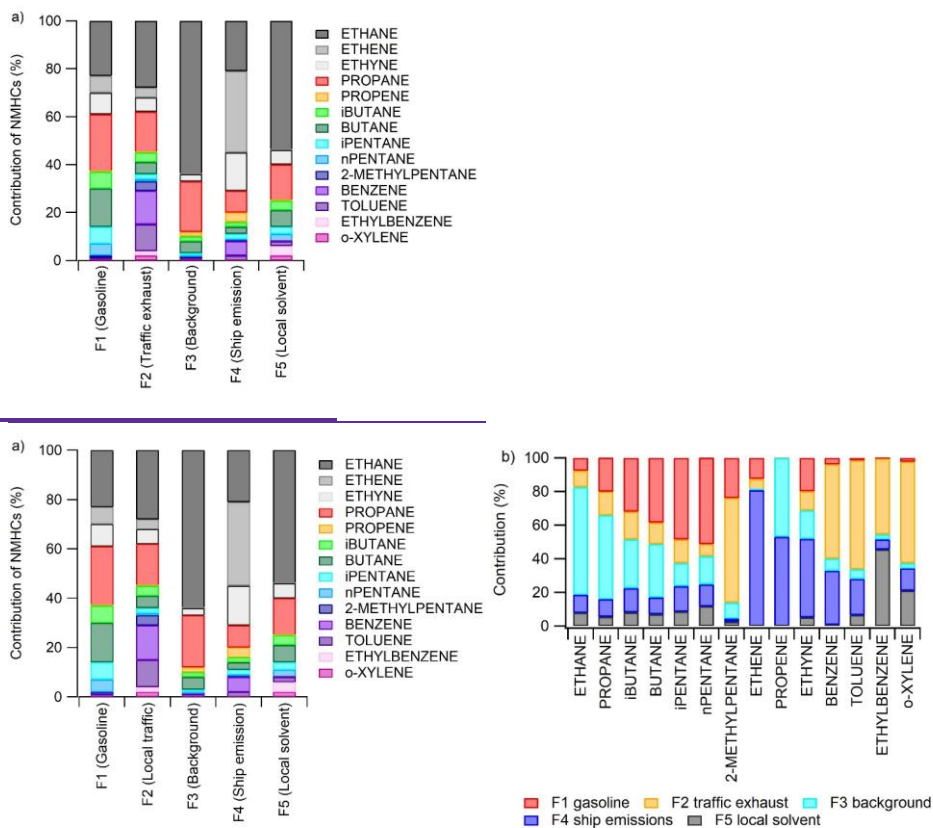


Figure 3: a) Relative contributions of compounds' mixing ratios in factors (% of factor sum) and b) relative contribution

335 of the factors on the average compound mixing ratios for the period of observations.

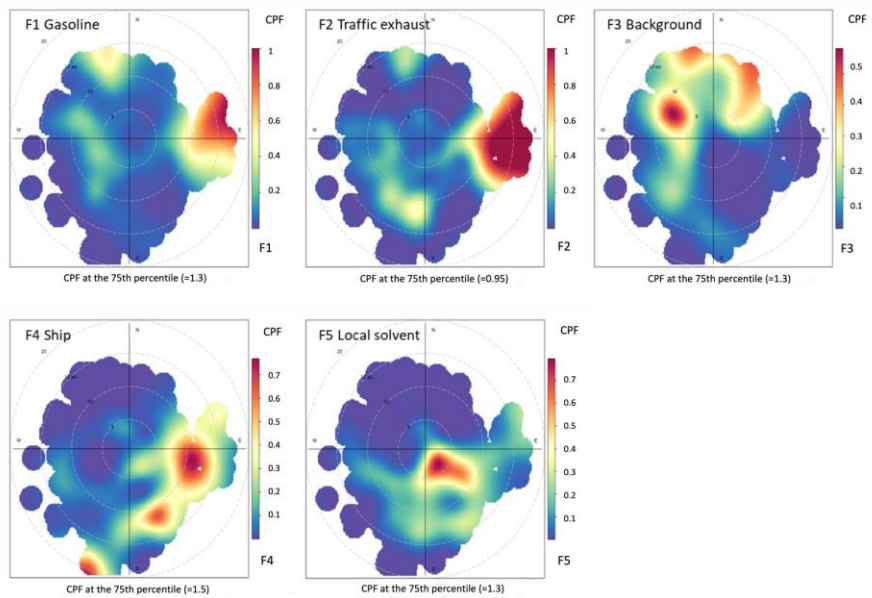
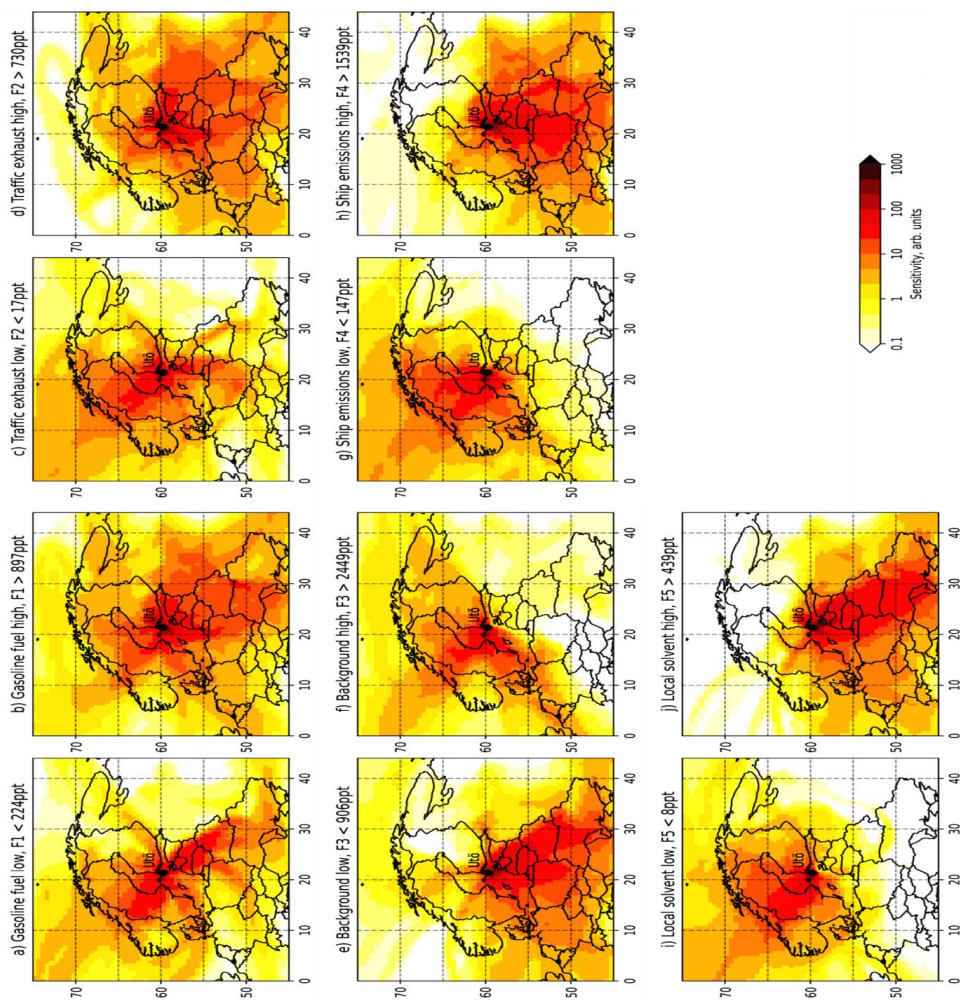
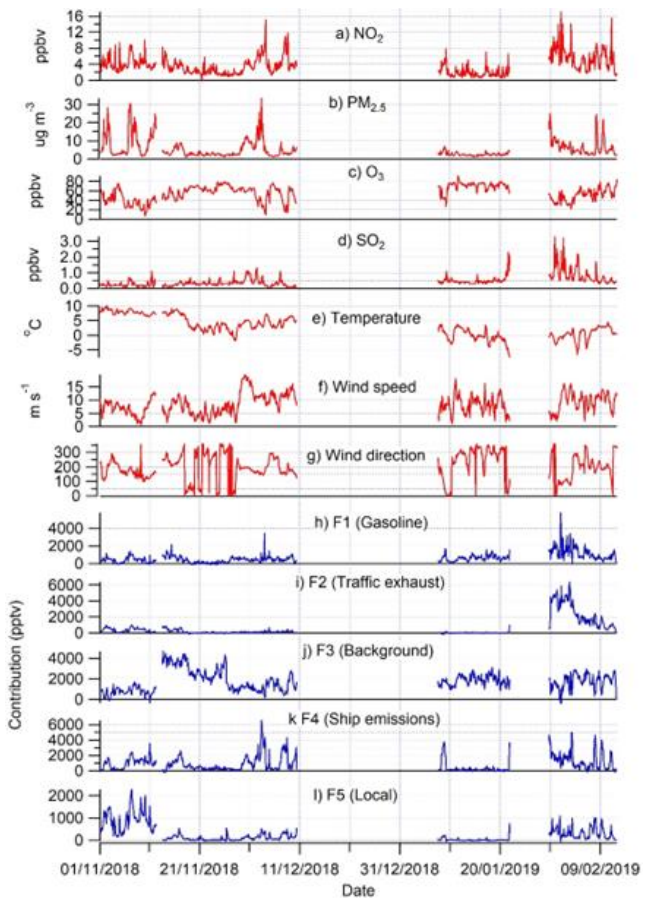


Figure 4: Probability function of distribution of wind direction and speed corresponding with the PMF factors. Dashed circles show the wind speed with 5 m/s increments.

Formatted: Not Highlight



345 **Figure 5: Sensitivity maps for “low” and “high” factor loadings showing the source area probabilities of factors (F1-F5).**



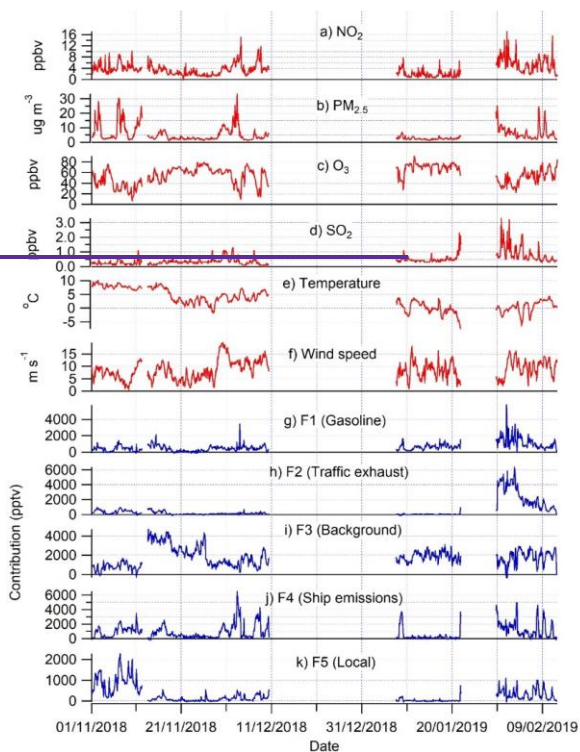


Figure 6: Time series of air pollutants (a-d, in red), meteorological parameters (e-fg, in red) and PMF factor contributions (gh-k, in blue) at Utö during the NMHC measurement periods in winter 2018-2019.

350

355 3.2.2 Sources of NMHCs

Based on the PMF analyses, the main source of studied NMHCs at Utö island was long-range transported air masses (F3) with a 42% contribution (Table 1). The strongest local/regional source was ship emissions F4 (21% contribution to the total NMHCs) followed by gasoline fuel (F1) and traffic exhaust emissions (F2) with 15% and 14% contributions, respectively. In

360 addition, there was a local solvent evaporation source (F5) with a 6% contribution.

Source contributions of individual NMHCs were highly variable (Fig. 3b). For lightest alkanes, ethane and propane, long-range transported background air was clearly the main source with 64% and 50% contributions, respectively. This is expected since compounds with long atmospheric lifetimes are known to accumulate in the atmosphere in northern latitudes during wintertime. Relatively high wintertime mixing ratios of them are detected even in remote areas (Hellén et al. 2015, Solberg et al. 2020). Gasoline fuel emissions (~35%) and background air (~30%) were major sources of butanes. For pentanes the main source was gasoline emissions with a ~50% contribution. For the alkane with shortest atmospheric lifetime, 2-methylpentane, traffic exhaust emissions were the main source with a 62% contribution.

Alkenes (ethene and propene) mainly originated from ship emissions with 81% and 53% contributions. For propene, long-range transported background air was also significant source with a 47% contribution. Due to the relatively short atmospheric lifetime of propene this is not expected. Uncertainties on defining a proper blank value for propene may have induced this. For other compounds, a blank was not detected or was not as significant. Ethyne was only alkyne detected and ship emissions were the major source for it with a 47% contribution.

For aromatic hydrocarbons, traffic exhaust emissions were the major source with 45-65% contributions. Based on the wind direction distribution, these emissions mainly originated from the east from the direction of the city of Saint Petersburg 500 km to the east from site. For benzene, toluene and o-xylene, ship emissions also resulted in 32%, 21% and 13% contributions, respectively. In addition, local solvent emissions contributed to the mixing ratios of ethylbenzene and o-xylene with 46% and 21% contributions, respectively. Due to shorter lifetime, these compounds have very low mixing ratios in remote areas and therefore as expected long-range transported background air did not result in a strong contribution.

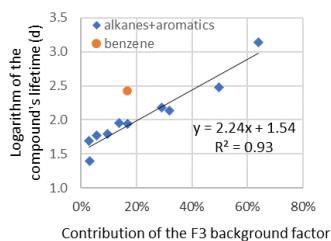


Figure 7: Correlation of the logarithm of a compound's lifetime (Hellén et al. 2015) with the contribution of the F3 background factor to the mixing ratio of the compound.

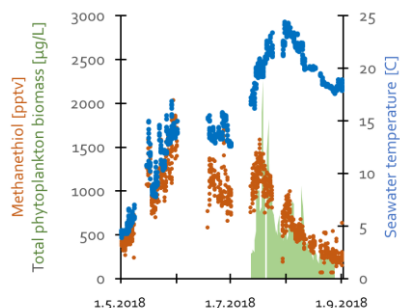
For alkanes and aromatic hydrocarbons, the loading of background factor F3 had a clear correlation ($R^2=0.93$) with the logarithm of the compound's lifetime (Fig.7). As expected, for compounds with the longest lifetime the contribution was highest. However, based on benzene lifetime, a stronger impact of the background air would have been expected. A higher

contribution of background air masses on benzene mixing ratios has been found even in the city of Helsinki in Finland (Hellén et al. 2006). This could indicate a stronger local source. However, the mixing ratios of benzene were not high, and it had low signal to noise ratio and therefore high uncertainties in the PMF solution and measurements of benzene were expected.

3.3 Mixing ratios of methanethiol

In addition to the NMHCs, we also detected methanethiol. Contrary to the usual annual cycle of anthropogenic VOCs, methanethiol had a maximum during spring and summer (Fig 2). Therefore, it is expected to have a biogenic origin. In earlier studies methanethiol has been detected, for example in phytoplankton and oceanic emissions (Kilgour et al. 2022, Novak et al. 2022). It is formed in the seawater from the same precursor metabolite, dimethyl sulfoniopropionate (DMSP), as DMS (Kiene and Linn, 2000).

At Utö, methanethiol mixing ratios started to increase in the end of April when the daily mean ambient air and seawater temperatures were above 5 and 4°C, respectively (Fig. 8a). The mixing ratios increased following changes in seawater temperature in spring and. The maximum mixing ratios were measured at the end of May. After mid July, the mixing ratios started to decrease even though seawater temperature still increased (Fig. 8a). The mixing ratios declined below detection limits in September. Total phytoplankton biomass in seawater was measured concurrent with the atmospheric VOCs during July-August and it is plotted together with methanethiol in Fig. 8b. Unfortunately, we do not have phytoplankton data from early summer due to instrument underwater pump failure. There are many factors that affect the removal of substances from water to air and dilutions of emissions in the air, but the methanethiol mixing ratios seem to follow the total phytoplankton biomass in seawater and the decrease in phytoplankton biomass may explain the decrease in the mixing ratios after mid-July.



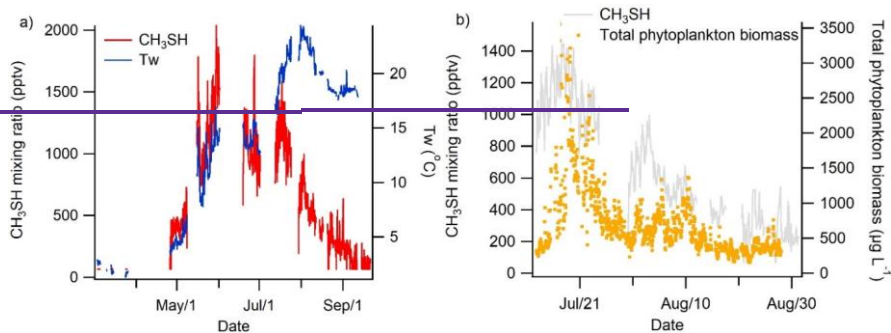
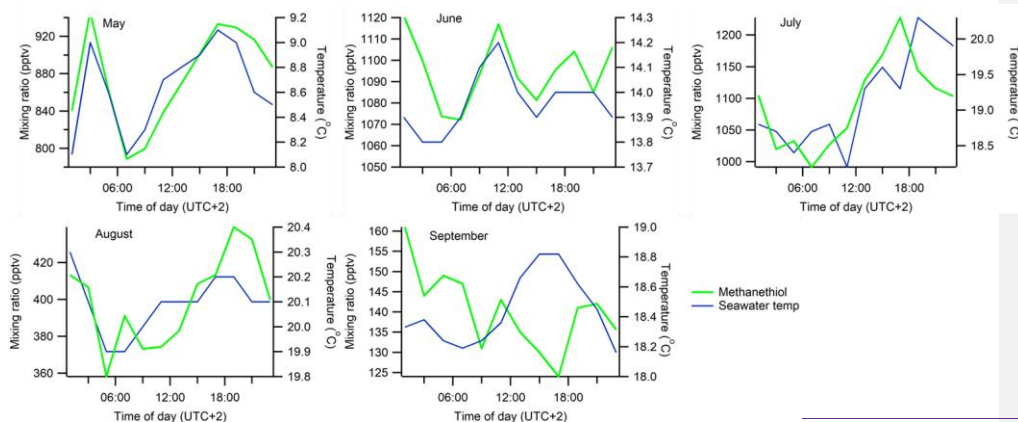


Figure 8: Methanethiol (CH₃SH) mixing ratios together with a) seawater temperature (Tw) in March-May - September August and b) total phytoplankton biomass in July - August 2018 at Utö.

415

The diurnal variation of the methanethiol mixing ratios followed the variation of the seawater temperature except in September, when mixing ratios were already close to the detection limit (Fig. 9). During the daytime, sink through OH oxidation is much higher than during the night. In addition, the mixing of layer heights in the atmosphere are expected to be clearly higher during the day resulting in higher dilution of emitted methanethiol during the daytime. Since the highest mixing ratios were still measured during the daytime, methanethiol is expected to have a very strong daytime emission source compared to nighttime emission. Light induced emissions could explain this. However, no correlation with radiation was found.

420

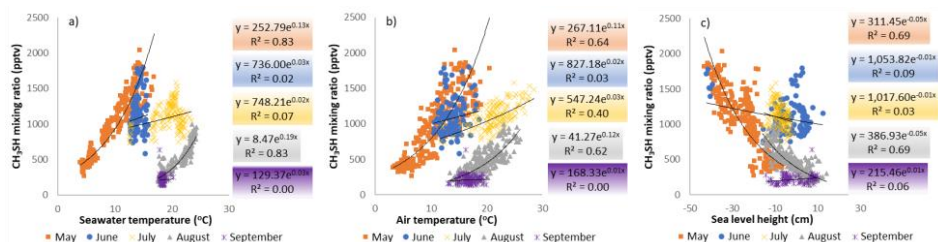


425 **Figure 9: Monthly mean diurnal variation of the methanethiol mixing ratios and seawater temperatures.**

Biogenic emissions of volatile organic compounds from vegetation are generally known to have exponential dependence on air/leaf/needle temperature (Guenther et al. 2012). Here, dependence of the mixing ratios of methanethiol on both ambient air and seawater temperatures were studied (Fig. 10). Even if phytoplankton would be the source of the ambient air methanethiol, temperature may be significant factor controlling its production by phytoplankton and its transfer from sea to atmosphere. The temperature dependence of the methanethiol mixing ratios varied over the season. In May, strong exponential dependence both on seawater ($R^2=0.83$) and ambient air ($R^2=0.65$) temperatures were found. In June, the mixing ratios did not correlate with seawater or ambient air temperatures ($R^2=0.02$ and 0.03 , respectively). However, the measurements were within quite a narrow temperature range. In July, there was some dependence with ambient air ($R^2=0.4$), but no correlation with seawater temperature ($R^2=0.07$). In August, the correlation of the mixing ratios with seawater and ambient air temperatures was again high with R^2 being 0.83 and 0.62 , respectively. The reason for these differences could be shifts in phytoplankton community composition and their physiological status, possible contributions from macroalgae vegetation from shoreline, and meteorology.

In addition to temperature, sea level height had a clear negative correlation with the methanethiol mixing ratios especially in May ($R^2=0.69$) and August ($R^2=0.69$, Fig. 10c). With lower sea levels, more macroalgae may be exposed to the ambient air and start decaying faster inducing more methanethiol emissions. This strong negative correlation could indicate macroalgae being a significant source of methanethiol. In June and July there was no correlation with sea level height, which indicates that other sources (e.g., phytoplankton) played a more important role. While seawater and ambient air temperature dependencies (Fig 10 a and b) were different for May and August, sea level height followed the same curve during both months (Fig 10 c).

445 The wind direction distribution (Fig. 11) indicates that the highest mixing ratios of methanethiol were measured during northerly winds ($5 - 10 \text{ m s}^{-1}$). To the north of the site, there are wide archipelago areas with frequently occurring phytoplankton blooms and macroalgae as possible sources of methanethiol.



Formatted: Left

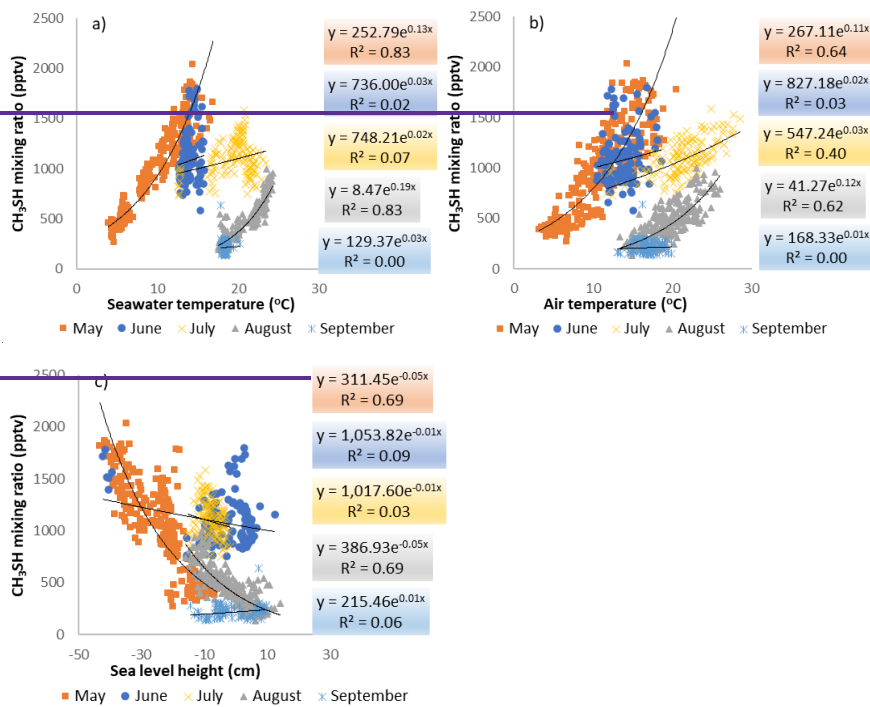


Figure 10: Dependence of methanethiol (CH₃SH) mixing ratios on a) seawater temperature, b) ambient air temperature and c) sea level height.

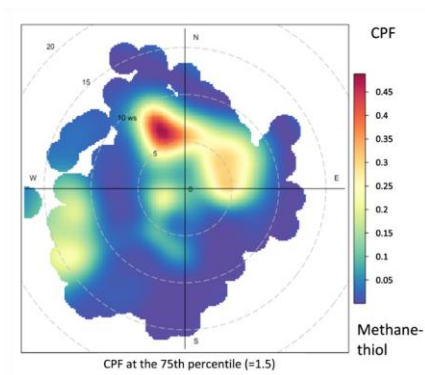


Figure 11: Probability function of distribution of wind direction and speed for the measured methanethiol mixing ratios. Dashed circles show the wind speed with 5 m/s increments.
 460 ~~Wind direction distribution for the measured methanethiol mixing ratios.~~

There is very little information available on methanethiol mixing ratios or emissions globally. Novak et al. (2022) measured a mean mixing ratio of 19 pptv at the Scripps Institution of Oceanography in La Jolla, CA, USA, during September 2019. The highest measured value was 217 pptv. Lawson et al. (2020) measured a mean mixing ratio of 18 pptv in the remote southwestern Pacific Ocean in the summer of 2012. These values are clearly lower than measured in this study in the Baltic Sea where highest monthly means were ~1000 pptv. The coastal location with the adjacent macroalgae vegetation and high production of phytoplankton in the nutrient rich and eutrophied Baltic Sea may explain these higher values.

Leck and Rodhe (1991) found 15 times higher DMS concentrations compared to methanethiol in seawater in the Baltic Sea. Here we did not detect DMS, but our method was not optimized for it, and it is possible that we do not capture it with our method.

Methanethiol is intensively malodorous. It has an odour threshold of 1000-2000 pptv. During warm weather with intensive phytoplankton blooms and decaying macroalgae on the shores of the island, the inhabitants of Utö are known to suffer from a very bad smell. In our measurements, the odour threshold was exceeded often in the summer of 2018.

Novak et al. (2022) found that methanethiol emissions are dependent on wind speed, but in this study, we did not find any correlation of mixing ratios with wind speed. While wind might increase emissions, it also increases dilution in the air. In addition, there are several other factors that impact the mixing ratios, e.g., oxidation and mixing layer height, and therefore emissions and the factors impacting them are not expected to be directly comparable with mixing ratios.

480 ~~In the atmosphere methanethiol oxidizes with OH radicals seven times faster than DMS (Kilgour et al. 2022). OH oxidation of methanethiol produces SO₂ with almost unity yield (Novak et al. 2022).~~ It has been estimated that methanethiol could be a source of up to 30% of the SO₂ formed in the marine boundary layer in coastal California, where clearly lower mixing ratios were measured than in this study (Novanak et al. 2022). In our study the methanethiol mixing ratios were high over several months and not just during short blooming periods (Fig. 2). This indicates that methanethiol could have a stronger contribution on SO₂ production in this area. More studies on methanethiol emissions ~~are would be~~ needed to confirm this.

485 **4 Conclusions**

The ambient air mixing ratios of NMHCs and methanethiol were studied at the marine research station on Utö island in the Baltic Sea. The NMHC mixing ratios were typical for the northern rural/remote site. The seasonal variations of NMHCs
490 followed a well-known cycle with maximum mixing ratios in winter and minimum during summer. The exception was methanethiol, which was identified here for the first time. It had a clear maximum in spring and summer.

Especially for longer living NMHCs, the regional background was shown to be the major source. The contribution of the background had an exponential correlation with the lifetime of the measured alkanes and aromatic hydrocarbons. This gives confidence that PMF can produce valid information on the source apportionment of NMHCs also at rural/remote sites, where
495 the ratios of these reactive compounds have been altered during transport from their sources to the site.

Of the local/regional sources, shipping had a strong impact especially on ethene, propene, ethyne and benzene. For shorter living NMHCs (aromatic hydrocarbons and 2-methylpentane), traffic emissions had major effect. Wind distribution analyses indicated that these traffic emissions came from the direction of the main harbours/cities of the Gulf of Finland including the city of Saint Petersburg 500 km to the east of site. Gasoline evaporative emissions originating in the east had a strong impact
500 on butane and pentane levels.

The mixing ratios of methanethiol followed the variations of seawater temperatures ~~from the end of April until mid July in spring and autumn. After that~~ After mid-July the mixing ratios started to decline while seawater temperatures remained high. ~~The diurnal variation of the mixing ratios still followed the variation of the temperatures.~~ During that time the abundance of phytoplankton in the seawater also declined ~~indicating phytoplankton as a possible source~~. The mixing ratios also negatively
505 correlated with sea level height especially in May and August. Macroalgae exposed to ambient air during low sea levels may start decaying faster and induce methanethiol emissions. ~~This-These~~ together with ambient air temperature dependence ~~and~~ high summertime mixing ratios ~~and correlation with phytoplankton abundance indicated gave indication on~~ the biogenic origin of methanethiol possible resulting from phytoplankton or macroalgae. The detected mixing ratios were higher than found earlier in other areas and may be the source of the malodour detected on the island during strong phytoplankton blooms. This
510 may also have strong impacts on local SO₂ production and new particle formation. More studies on methanethiol emissions and atmospheric impacts ~~would be are~~ needed ~~to confirm these findings~~.

Competing interests: The contact author has declared that none of the authors has any competing interests.

515 **Acknowledgements:** The observations at Utö were supported by Academy of Finland project SEASINK (grants # 317297&
317298), Finnish marine research infrastructure (FINMARI) and the JERICO-S3 project, funded by the European
Commission's H2020 Framework Programme under grant agreement No. 871153. JPJ would like to acknowledge the funding
from the EU H2020 project EMERGE, which received funding from the European Union's Horizon 2020 Research and
Innovation Programme under grant agreement no. 874990 (EMERGE project). Timo Mäkelä and Juha Hatakka are thanked
520 for their help on setting up the measurements. Milla Johansson is thanked for providing sea level height data. Simo-Matti Siiriä
is acknowledged for drawing the Fig. 1.

References

- Anderson M., Salo K. and Fridell E.: Particle- and Gaseous Emissions from an LNG Powered Ship, *Environmental Science and Technology*, 49, 12568-12575, <https://doi.org/10.1021/acs.est.5b02678>, 2015.
- 525 Boursoukoudis, E., Ernle, L., Crowley, J. N., Lelieveld, J., Paris, J.-D., Pozzer, A., Walter, D., and Williams, J.: Non-methane hydrocarbon (C₂-C₈) sources and sinks around the Arabian Peninsula, *Atmos. Chem. Phys.*, 19, 7209–7232, <https://doi.org/10.5194/acp-19-7209-2019>, 2019.
- 530 Carslaw, D.C., 2018. Package “Openair.” Tools for the analysis of air pollution data. <http://davidcarslaw.github.io/openair/>.
- Castano, N. P., Ramirez, V., and Cancelado, J.A.: Controlling Painters' Exposure to Volatile Organic Solvents in the automotive Sector of Southern Colombia, *Safety and Health Work*, 10, 355-361, <https://doi.org/10.1016/j.shaw.2019.06.001>, 2019.
- 535 CEN (2015) DIN EN 16695 water quality – guidance on the estimation of phytoplankton biovolume: English version EN 16695, 2015. Available at: <https://standards.iteh.ai/catalog/standards/cen/bcc87031-164e-45b9-933a-7db83d4658f4/en-16695-2015> (Accessed July 9, 2020).
- 540 Edtbauer, A., Stöner, C., Pfannerstill, E. Y., Berasategui, M., Walter, D., Crowley, J. N., Lelieveld, J., and Williams, J.: A new marine biogenic emission: methane sulfonamide (MSAM), dimethyl sulfide (DMS), and dimethyl sulfone (DMSO₂) measured in air over the Arabian Sea, *Atmos. Chem. Phys.*, 20, 6081–6094, <https://doi.org/10.5194/acp-20-6081-2020>, 2020.
- [EMEP emission database. https://www.ceip.at/webdab-emission-database](https://www.ceip.at/webdab-emission-database), last accessed 9.10.2023.

545

Ge, Y., Solberg, S., Heal, M., Reimann, S., van Caspel, W., Hellack, B., Salameh, T., and Simpson, D.: Evaluation of modelled versus observed NMVOC compounds at EMEP sites in Europe, *EGUsphere* [preprint], <https://doi.org/10.5194/egusphere-2023-3102>, 2024.

550 Guenther, A. B., Jiang, X., Heald, C. L., Sakulyanontvittaya, T., Duhl, T., Emmons, L. K., and Wang, X.: The Model of Emissions of Gases and Aerosols from Nature version 2.1 (MEGAN2.1): an extended and updated framework for modelling biogenic emissions, *Geosci. Model Dev.*, 5, 1471–1492, <https://doi.org/10.5194/gmd-5-1471-2012>, 2012.

Hakola, H., Hellén, H. and Laurila, T.: Ten years of light hydrocarbons (C₂–C₆) concentration measurements in background
555 air in Finland, *Atmospheric Environment* 40, 3621–3630, 2006.

Hellén, H., Hakola, H., Pirjola, L., Laurila, T., and Pystynen, K.-H.: Ambient air concentrations, source profiles and source apportionment of 71 different C₂-C₁₀ volatile organic compounds in urban and residential areas of Finland, *Environmental Science and Technology*, 40, 103-108, 2006.

560

Hellén, H., Kouznetsov, R., Anttila, P., and Hakola, H.: Twenty years of NMHC measurements at Pallas-Sodankylä GAW station in Northern Finland; trends, source areas and short term variability, *Boreal Env. Res.* 20, 542-552, 2015.

Hersbach, H., Bell, B., Berrisford, P., Hirahara, S., Horányi, A., Muñoz-Sabater, J., Nicolas, J., Peubey, C., Radu, R., Schepers, D., Simmons, A., Soci, C., Abdalla, S., Abellan, X., Balsamo, G., Bechtold, P., Biavati, G., Bidlot, J., Bonavita, M., Chiara, G., Dahlgren, P., Dee, D., Diamantakis, M., Dragani, R., Flemming, J., Forbes, R., Fuentes, M., Geer, A., Haimberger, L., Healy, S., Hogan, R. J., Hólm, E., Janisková, M., Keeley, S., Laloyaux, P., Lopez, P., Lupu, C., Radnoti, G., Rosnay, P., Rozum, I., Vamborg, F., Villaume, S., and Thépaut, J.-N.: The ERA5 global reanalysis, *Q. J. Roy. Meteor. Soc.*, online first, <https://doi.org/10.1002/qj.3803>, 2020. [a](#), [b](#), [c](#)

570

Honkanen, M., Tuovinen, J-P., Laurila, T., Mäkelä, T., Hatakka, J., Kielosto, S., and Laakso, L.: [Measuring turbulent CO₂ fluxes with a closed-path gas analyzer in a marine environment](#), *Atmos. Meas. Tech.*, 11, 5335-5350, <https://doi.org/10.5194/amt-11-5335-2018>, 2018.

575 Honkanen, M., Müller, J. D., Seppälä, J., Rehder, G., Kielosto, S., Ylöstalo, P., Mäkelä, T., Hatakka, J., and Laakso, L.: The diurnal cycle of pCO₂ in the coastal region of the Baltic Sea, *Ocean Sci.*, 17, 1657-1675, <https://doi.org/10.5194/os-17-1657-2021>, 2021.

- Honkanen, M., Aurela, M., Hatakka, J., Haraguchi, L., Kielosto, S., Mäkelä, T., Seppälä, J., Stenbäck, K., Tuovinen, J.-P.,
580 Ylöstalo, P. and Laakso, L., Observed interannual variability of the net CO₂ air-sea exchange in the coastal region of the Baltic
Sea, to be submitted, 2023.
- Hopke, P.: Review of receptor modeling methods for source apportionment, *J. Air Waste Manag. Assoc.*, 66, 237–259, 2016.
- 585 Hopke, P. K., Dai, Q., Li, L., and Feng, Y.: Global review of recent source apportionments for airborne particulate matter, *Sci.
Total Environ.*, 740, 2020.
- Jalkanen, J. P., Brink, A., Kalli, J., Pettersson, H., Kukkonen, J., & Stipa, T.: A modelling system for the exhaust emissions of
590 marine traffic and its application in the Baltic Sea area. *Atmospheric Chemistry and Physics*, 9(23), 9209–9223.
<https://doi.org/10.5194/acp-9-9209-2009>, 2009.
- Jalkanen, J.-P., Johansson, L., Kukkonen, J., Brink, A., Kalli, J., & Stipa, T.: Extension of an assessment model of ship traffic
exhaust emissions for particulate matter and carbon monoxide. *Atmospheric Chemistry and Physics*, 12(5), 2641–2659.
595 <https://doi.org/10.5194/acp-12-2641-2012>, 2012.
- Johansson, L., Jalkanen, J.-P., & Kukkonen, J.: Global assessment of shipping emissions in 2015 on a high spatial and temporal
resolution. *Atmospheric Environment*, 167, 403–415. <https://doi.org/10.1016/j.atmosenv.2017.08.042>, 2017.
- 600 Kahru, M., and Elmgren, R., Multidecadal time series of satellite-detected accumulations of cyanobacteria in the Baltic Sea,
Biogeosciences 11, 3619–3633, doi: 10.5194/bg-11-3619-2014, 2014.
- Kiene R. P., and Linn L. J.: Distribution and turnover of dissolved DMSP and its relationship with bacterial production and
dimethylsulfide in the Gulf of Mexico, *Limnol. Oceanogr.*, 45, 849–861, <https://doi.org/10.4319/lo.2000.45.4.0849>, 2000.
605
- Kilgour D. L., Novak G. A., Sauer J. S., Moore A. N., Dinasquet J., Amiri S., Franklin E. B., Mayer K., Winter M., Morris C.
K., Price T., Malfatti F., Crocker D. R., Lee C., Cappa C. D., Goldstein A. H., Prather K. A., and Bertram T. H.: Marine gas-
phase sulfur emissions during an induced phytoplankton Bloom, *Atmos. Chem. Phys.*, 22, 1601–1613,
<https://doi.org/10.5194/acp-2021-615>, 2022.
- 610 Kouznetsov, R., Sofiev, M., Vira, J., and Stiller, G.: Simulating age of air and the distribution of SF₆ in the stratosphere with
the SILAM model, *Atmos. Chem. Phys.*, 20, 5837–5859, <https://doi.org/10.5194/acp-20-5837-2020>, 2020.

Kraft, K., Seppälä, J., Hällfors, H., Suikkanen, S., Ylöstalo, P., Anglès, S., Kielosto, S., Kuosa, H., Laakso, L., Honkanen, M.,
615 Lehtinen, S., Oja, J., and Tamminen, T.: Application of IFCB High-Frequency Imaging-in-Flow Cytometry to Investigate
Bloom-Forming Filamentous Cyanobacteria in the Baltic Sea, <https://www.frontiersin.org/article/10.3389/fmars.2021.594144>,
Frontiers in Marine Science, 2021.

Kraft, K., Velhonoja, O., Eerola, T., Suikkanen, S., Tamminen, T., Haraguchi, L., Ylöstalo P., Kielosto S., Johansson, M.,
620 Lensu, L., Käviäinen H., Haario, H., and Seppälä, J.: Towards operational phytoplankton recognition with automated high-
throughput imaging, near-real-time data processing, and convolutional neural networks, *Frontiers in Marine Science*, 9,
867695, 2022.

Laakso, L., Mikkonen, S., Drebs, A., Karjalainen, A., Pirinen, P., and Alenius, P.: 100 years of atmospheric and marine
625 observations at the Finnish Utö Island in the Baltic Sea, *Ocean Sci.*, 14, 617–632, <https://doi.org/10.5194/os-14-617-2018>,
2018.

Lanz, V. A., Henne, S., Staehelin, J., Hueglin, C., Vollmer, M. K., Steinbacher, M., Buchmann, B., and Reimann, S.: Statistical
analysis of anthropogenic non-methane VOC variability at a European background location (Jungfrauoch, Switzerland),
630 *Atmos. Chem. Phys.*, 9, 3445–3459, doi:10.5194/acp-9-3445-2009, 2009.

Laurila, T. and Hakola, H.: Seasonal Cycle of C₂–C₅ hydrocarbons over the Baltic Sea and Northern Finland, *Atmospheric
Environment* 30, 1597-1607, 1996.

635 Lawson, S. J., Law, C. S., Harvey, M. J., Bell, T. G., Walker, C. F., de Bruyn, W. J., and Saltzman, E. S.: Methanethiol,
dimethyl sulfide and acetone over biologically productive waters in the southwest Pacific Ocean, *Atmos. Chem. Phys.*, 20,
3061–3078, <https://doi.org/10.5194/acp-20-3061-2020>, 2020.

Leck, C., and Rodhe, H.: Emissions of marine biogenic sulfur to the atmosphere of northern Europe, *Journal of Atmospheric
640 Chemistry*, 12, 63-86, 1991.

Leuchner, M., Gubo, S., Schunk, C., Wastl, C., Kirchner, M., Menzel, A., and Plass-Dülmer, C.: Can positive matrix
factorization help to understand patterns of organic trace gases at the continental Global Atmosphere Watch site
Hohenpeissenberg?, *Atmos. Chem. Phys.*, 15, 1221–1236, <https://doi.org/10.5194/acp-15-1221-2015>, 2015.

645

Meinander, O., Kazadzis, S., Arola, A., Riihelä, A., Räisänen, P., Kivi, R., Kontu, A., Kouznetsov, R., Sofiev, M., Svensson, J., Suokanerva, H., Aaltonen, V., Manninen, T., Roujean, J.-L., and Hautecoeur, O.: Spectral albedo of seasonal snow during intensive melt period at Sodankylä, beyond the Arctic Circle, *Atmos. Chem. Phys.*, 13, 3793–3810, <https://doi.org/10.5194/acp-13-3793-2013>, 2013.

650

Meinander, O., Kontu, A., Kouznetsov, R. and Sofiev, M.: Snow Samples Combined With Long-Range Transport Modeling to Reveal the Origin and Temporal Variability of Black Carbon in Seasonal Snow in Sodankylä (67°N), *Front. Earth Sci.*, 8, <https://doi.org/10.3389/feart.2020.00153>, 2020.

655

Moberg, E. A., and Sosik, H. M.: Distance maps to estimate cell volume from two-dimensional plankton images, *Limnol. Oceanogr. Methods* 10, 278–288, doi: 10.4319/lom.2012.10.278, 2012.

Novak, G. A., Kilgour, D. B., Jernigan, C. M., Vermeuel, M. P., and Bertram, T. H.: Oceanic emissions of dimethyl sulfide and methanethiol and their contribution to sulfur dioxide production in the marine atmosphere, *Atmos. Chem. Phys.*, 22, 6309–

660

6325, <https://doi.org/10.5194/acp-22-6309-2022>, 2022.

Petersen, A. K., Brasseur, G. P., Bouarar, I., Flemming, J., Gauss, M., Jiang, F., Kouznetsov, R., Kranenburg, R., Mijling, B., Peuch, V.-H., Pommier, M., Segers, A., Sofiev, M., Timmermans, R., van der A, R., Walters, S., Xie, Y., Xu, J., and Zhou, G.: Ensemble forecasts of air quality in eastern China – Part 2: Evaluation of the MarcoPolo–Panda prediction system, version

665

1, *Geosci. Model Dev.*, 12, 1241–1266, <https://doi.org/10.5194/gmd-12-1241-2019>, 2019.

Polissar, A.V., Hopke, P. K., Paatero, P., Malm, W.C. and Sisler, J.F.: Atmospheric aerosol over Alaska 2. Elemental composition and sources. *J. Geophys. Res.*, 103(D15): 19045-19057, 1998.

670

Rautiainen, L., Tyynelä, J., Lensu, M., Siiriä, S., Vakkari, V., O'Connor, E., Hämäläinen, K., Lonka, H., Stenbäck, K., Koistinen, J. and Laakso, L.: Utö Observatory for Analysing Atmospheric Ducting Events over Baltic Coastal and Marine Waters, *Remote Sens.*, 15, <https://doi.org/10.3390/rs15122989>, 2023.

Sauvage, S., Plaisance, H., Locoge, N., Wroblewski, A., Coddeville, P., and Galloo, J. C.: Long term measurement and source

675

apportionment of non-methane hydrocarbons in three French rural areas, *Atmos. Environ.*, 43, 2430–2441, doi:10.1016/j.atmosenv.2009.02.001, 2009.

Sofiev, M., Vira, J., Kouznetsov, R., Prank, M., Soares, J., and Genikhovich, E.: Construction of the SILAM Eulerian atmospheric dispersion model based on the advection algorithm of Michael Galperin, *Geosci. Model Dev.*, 8, 3497–3522, <https://doi.org/10.5194/gmd-8-3497-2015>, 2015.

Sofiev, M., Winebrake, J.J., Johansson, L., Carr E.W., Prank M., Soares J., Vira J., Kouznetsov R., Jalkanen j.-p., Corbett J.J.: Cleaner fuels for ships provide public health benefits with climate trade-offs. *Nature Communications*, 9, 406, <https://doi.org/10.1038/s41467-017-02774-9>, 2018.

Solberg S., Claude A., Reimann S., Sauvage S.: VOC measurements 2018. EMEP/CCC-Report 4/2020, <https://hdl.handle.net/11250/2677930>, 2020.

Song M. Y. and Chun H.: Species and characteristics of volatile organic compounds emitted from an auto-repair painting workshop, *Scientific reports*, 11, 16586, <https://doi.org/10.1038/s41598-021-96163-4>, 2021.

Sun, X., Wang, H., Guo, Z., Lu, P., Song, F., Liu, L., Liu, J., Rose, N.L., and Wang, F.: Positive matrix factorization on source apportionment for typical pollutants in different environmental media: a review, *Environ. Sci.: Processes Impacts*, 22, 239, DOI: 10.1039/c9em00529c, 2020.

Tang, L., Ramacher, M. O. P., Moldanová, J., Matthias, V., Karl, M., Johansson, L., Jalkanen, J.-P., Yaramenka, K., Aulinger, A., and Gustafsson, M.: The impact of ship emissions on air quality and human health in the Gothenburg area – Part 1: 2012 emissions, *Atmos. Chem. Phys.*, 20, 7509–7530, <https://doi.org/10.5194/acp-20-7509-2020>, 2020.

Thames, A. B., Brune, W. H., Miller, D. O., Allen, H. M., Apel, E. C., Blake, D. R., Bui, T. P., Commane, R., Crouse, J. D., Daube, B. C., Diskin, G. S., DiGangi, J. P., Elkins, J. W., Hall, S. R., Hanisco, T. F., Hannun, R. A., Hintsä, E., Hornbrook, R. S., Kim, M. J., McKain, K., Moore, F. L., Nicely, J. M., Peischl, J., Ryerson, T. B., St. Clair, J. M., Sweeney, C., Teng, A., Thompson, C. R., Ullmann, K., Wennberg, P. O., and Wolfe, G. M.: Missing OH reactivity in the global marine boundary layer, *Atmos. Chem. Phys.*, 20, 4013–4029, <https://doi.org/10.5194/acp-20-4013-2020>, 2020.

Vestenius M., Hopke P. K., Lehtipalo K., Petäjä T., Hakola H., and Hellén H.: Assessing volatile organic compound sources in a boreal forest using positive matrix factorization (PMF), *Atmospheric Environment*, 259, <https://doi.org/10.1016/j.atmosenv.2021.118503>, 2021.

Formatted: Font: Not Italic

Formatted: Font: Not Italic

Formatted: Font: Not Bold

Formatted: English (United Kingdom)

Viana, M., Hammingh, P., Colette, A., Querol, X., Degraeuwe, B., de Vlieger, I., and Van Aardenne, J: Impact of maritime transport emissions on coastal air quality in Europe, *Atmos. Environ.*, 90, 96–105, 2014.

715 Wang, M., Li, S., Zhu, R., Zhang, R., Zu, L., Wang, Y., and Bao, X.: On-road tailpipe emission characteristics and ozone formation potentials of VOCs from gasoline, diesel and liquefied petroleum gas fueled vehicles, *Atmospheric Environment*, 223, 117294, <https://doi.org/10.1016/j.atmosenv.2020.117294>, 2020.

[Watson S.B. and Jüttner F.: Malodorous volatile organic sulfur compounds: Sources, sinks and significance in inland waters. *Critical Reviews in Microbiology*, 43:2, 210-237, DOI: 10.1080/1040841X.2016.1198306, 2017.](#)

720

Wu, D., Fei, L., Zhang, Z., Zhang, Y., Li, Y., Chan, C., Wang, X., Cen, C., Li, P. and Yu, L.: Environmental and Health Impacts of the Change in NMHCs Caused by the Usage of Clean Alternative Fuels for Vehicles, *Aerosol Air Qual. Res.*, 20:930-943. <https://doi.org/10.4209/aaqr.2019.09.0459>, 2020a.

725

Wu, Z., Zhang, Y., He, J., Chen, H., Huang, X., Wang, Y., Yu, X., Yang, W., Zhang, R., Zhu, M., Li, S., Fang, H., Zhang, Z., and Wang, X.: Dramatic increase in reactive volatile organic compound (VOC) emissions from ships at berth after implementing the fuel switch policy in the Pearl River Delta Emission Control Area, *Atmos. Chem. Phys.*, 20, 1887–1900, <https://doi.org/10.5194/acp-20-1887-2020>, 2020b.

730

[Yu, Z. and Li, Y.: Marine volatile organic compounds and their impacts on marine aerosol – A review. *Sci. Total Environ.*, 768, 145054, <https://doi.org/10.1016/j.scitotenv.2021.145054>, 2021.](#)

Formatted: English (United Kingdom)

735 Yuan, B., Shao, M., de Gouw, J., Parrish, D. D., Lu, S., Wang, M., Zeng, L., Zhang, Q., Song, Y., Zhang, J., and Hu, M.: Volatile organic compounds (VOCs) in urban air: how chemistry affects the interpretation of positive matrix factorization (PMF) analysis, *J. Geophys. Res.*, 117, D24302, 1–17, doi:10.1029/2012JD018236, 2012.